

2004.  
30) Meylan, E. et al. : *Nature*, **437** : 1167-1172, 2005.  
31) Cheng, G. et al. : *Proc. Natl. Acad. Sci. USA*, **103** :  
8499-8504, 2006.

- 32) Loo, Y.M. et al. : *Proc. Natl. Acad. Sci. USA*, **103** :  
6001-6006, 2006.  
33) Paeshuyse, J. et al. : *Hepatology*, **43** : 761-770, 2006.

# 新しい 分子生物学の手法

第  
16  
回

## C型肝炎ウイルス

脇田隆宇\*



- ①C型肝炎ウイルス(HCV)は慢性肝疾患の原因ウイルスである。
- ②HCVはウイルス培養が困難なために、治療法や予防法の開発が遅れていた。
- ④レプリコンやシュードタイプウイルスなどの開発により、HCV研究は進行してきた。
- ⑤遺伝子型2aのJFH-1株によるウイルス培養系の開発に成功した。

Key Words/HCV, レプリコン, シュードタイプウイルス, ウイルス培養, JFH-1

### ● はじめに

B型肝炎ウイルスとA型肝炎ウイルスが相次いで発見された後も、原因ウイルスがわからないウイルス性肝炎患者が存在した。そして非A非B型肝炎として、その原因ウイルスの探索が長くおこなわれた。1989年に米国カイロン社の研究グループによりC型肝炎ウイルス(HCV)と命名されたが、従来のウイルス学的方法では検出できず、このウイルスは分子生物学的手法によりそのcDNAが同定された<sup>1)</sup>。ウイルス遺伝子が完全にクローニングされた後も実験室内でウイルスを培養することはできず、ウイルスの感染複製機構や病原性の解明は困難であった。さらに抗ウイルス薬の開発の遅れにもつながった。しかし、最近、HCVに対してさまざまな特徴のある研究方法が開発された(表①)。本稿ではHCVのウイルス学的研究の最近の話題について述べる。

### ① 感染性 cDNA クローン

HCVは約9.6 kbのプラス鎖RNAをゲノムにもつが、ウイルスゲノムcDNAは3'末端の3'X領域が同定されて完全長がクローニングされた。HCVはゲノムの多様性を特徴としているため、ウイルスの複製活性が保持されている配列を同定することが困難であった。このため、患者血清からクローニングされた複数のクローンを混合してチンパンジーに投与することにより感染性cDNAクローンの配列が決定された<sup>2)</sup>。チンパンジーには感染性があることが確認されたが、培養細胞では複製が困難であった。

### ② HCV レプリコン

1999年にドイツのバーテンシュレージャー博士らがHCVのレプリコン実験系を開発した<sup>3)</sup>。このレプリコンによって培養細胞で、ウイルス遺伝子複製機構の解析がはじめて可能になった。以前に報告された、ほかのウイ

\* WAKITA Takaji/国立感染症研究所・ウイルス第二部

表① C型肝炎ウイルスの実験系(筆者作成)

実験系	RNA複製	ウイルス粒子形成	感染
レプリコン	○	×	×
シュードタイプウイルス	×	△*	○
JFH-1株による感染系	○	○	○

\*レトロウイルスの表面にHCVのE1およびE2蛋白質が発現している。

ルスのRNAレプリコンと類似の方法で作製された。ウイルス粒子を形成する構造領域遺伝子を取り除き、ネオマイシン耐性遺伝子とEMCVのIRESを挿入してレプリコンを構築した。試験管内で合成したレプリコンRNAをHuh7細胞に導入し、G418存在下で培養した。レプリコンRNAが複製増殖している細胞はネオマイシン耐性遺伝子が発現するために生存するが、それ以外の細胞は死滅する。

最初に報告されたレプリコンは遺伝子型1bのCon1株を用いたレプリコンであった。興味深いことにレプリコンRNAが複製している細胞からレプリコンRNAを分離してその配列を解析すると、元々の配列とは異なる変異が存在することがわかった。変異は単一ではなく、そのなかにはレプリコンの複製効率を増強するものが存在した<sup>4)</sup>。このような変異をadaptive mutation(適合変異)とよび、適合変異を組み合わせることでさらに複製効率がよくなる場合があることもわかった<sup>5)</sup>。しかし、これらの変異は感染患者から分離されるウイルス遺伝子にはまったくみられなかった。HCVレプリコンはしばらく遺伝子型1bのCon1株でしか成功しなかったが、適合変異を導入したり、レプリコン細胞をインターフェロンでレスキューすることにより得られたcured cellを用いることにより、ほかのウイルス株でもレプリコン増殖が可能になった<sup>6)</sup>。

レプリコンでウイルスRNAの複製増殖が可能となったので、ウイルス粒子形成や感染増殖を可能とするためにウイルスの構造領域遺伝子を導入した全長のウイルスゲノムをもつレプリコンが作製された。遺伝子型1bのCon1株、N株および遺伝子型1aのH77株の全長レプリコンが報告されている。いずれのウイルス株のレプリコンも全長遺伝子の複製が確認されたが、ウイルス粒子の産生および培養液中への分泌は確認されなかった。さ

らに、適合変異を導入した全長ウイルスゲノムはチンパンジーに対して感染性がなかった。

### ③ ウイルスの精製表面蛋白質の結合実験系とシュードタイプウイルス

前述のとおり、レプリコンは細胞内でのウイルスゲノム複製に関する実験系であるが、ウイルス粒子の形成および分泌は観察できず、感染過程の解析はできなかった。そこで、ウイルスの感染初期過程においてウイルスと標的細胞の結合を解析するために、ウイルスの表面蛋白質を精製して標的細胞に結合させることが試みられた。この実験系からCD81という分子がHCVのE2蛋白質に結合することが明らかとなった。しかしこの実験系ではウイルス蛋白質の細胞表面への結合以降の段階を解析できない。そこで、HCVの感染過程をさらに解析するためにHCVの表面蛋白質をもつシュードタイプウイルスが開発された。HCVの表面蛋白質はER retention signalをもつため、細胞表面には発現しない。このためVSVによるシュードタイプウイルスを作製する際にはE1、E2蛋白質が細胞表面に発現するようにした。この結果感染にはE1、E2両方の表面蛋白質が必要であることが判明したが、CD81の発現していないHepG2細胞で感染可能であったため、CD81非依存性の感染と考えられた<sup>7)</sup>。

さらにE1、E2蛋白質を修飾せずにnativeなまま発現させ、レトロウイルスを用いてシュードウイルスが作製された<sup>8)</sup>。HCVのE1、E2蛋白質をもつシュードウイルスはCD81依存性の感染性を示した。CD81を発現するHuh7細胞には感染性があつたが、CD81を発現しないHepG2細胞には感染性を示さなかった。さらに、HepG2細胞にCD81を強制発現させた細胞は感染性を獲得した。また、スカベンジャーレセプターである

SR-B1 が感染に重要であることが示された。

#### ④ 遺伝子型 2a の JFH-1 株の分離とウイルス培養系の開発

われわれは HCV 感染ではまれな病態である劇症肝炎患者から HCV 株をクローニングして JFH-1 株と名づけた<sup>9)</sup>。JFH-1 株の特徴は①遺伝子型 2a であること、②モノクローンであること、③慢性肝炎患者から分離されたほかの遺伝子型 2a のウイルス株と比較すると遺伝子配列に変異が多いことであった。この JFH-1 株の培養細胞での複製効率を検討するためにサブジェノミックレプリコンを作製した。JFH-1 株のレプリコンは Con1 株のレプリコンよりもコロニー形成効率がよいことが明らかとなった<sup>10)</sup>。さらに既報のレプリコンは Huh7 細胞のみで複製が可能であったが、JFH-1 株のレプリコンは肝臓由来のほかの培養細胞や、肝臓以外の臓器由来の培養細胞でも複製が可能であった<sup>11)12)</sup>。したがって、HCV の複製には肝臓特異的な因子が必ずしも必要ではないことが示唆された。

さらに JFH-1 株の全長 cDNA から全長ウイルス RNA を合成して Huh7 細胞に導入するとウイルスゲノムが複製増殖することがわかった<sup>13)</sup>。ウイルスゲノムが複製している細胞ではウイルス粒子が形成されて培養液中に分泌された。このリコンビナントウイルス粒子は密度勾配遠心による分析により密度が 1.15 ~ 1.17 g/mL であり、RNase 抵抗性であった。さらに電子顕微鏡による解析で直径約 60 nm であった。このウイルス粒子は新たな Huh7 細胞に感染性があり、さらにレプリコンの複製感受性を高めた cured cell に感染することによりほぼ 100% の細胞に感染が可能となった<sup>14)</sup>。ウイルス感染による細胞障害は感染初期にはみられないが、感染が全細胞に広がると感染細胞が死滅する場合がある。しかし、つねにウイルス感染による細胞障害がみられるわけではないため、感染力価の測定には感染フォーカスの測定による。

培養細胞で作製されたりコンビナントウイルスの感染は、レトロタイプのシュードウイルスと同様に CD81 に依存していた。CD81 に対する抗体で培養細胞を処理することにより、感染は阻止される。さらに、この感染は

ウイルスの E2 蛋白質に対する抗体で阻止できた。また、チンパンジーによる感染実験により、培養液中に分泌されたりコンビナントウイルスの *in vivo* における感染性も確認できた。

#### ⑤ JFH-1 株以外の感染性ウイルス

H77 株は遺伝子型 1a で、レプリコンによる解析により、効率のよい複製には複数の適合変異が必要であった。適合変異を導入した、H77 株の全長遺伝子構築を用いて、合成 RNA からウイルス粒子の作製を試みた。合成 RNA の Huh7.5 細胞への導入により、感染性のウイルス粒子が分泌されることが証明された<sup>15)</sup>。JFH-1 株よりも効率は悪いが、同様の手法により感染性ウイルスが産生可能であることは重要である。また、JFH-1 株の構造領域をほかのウイルス株に入れ替えたキメラウイルスが作製された。これらのキメラウイルスの表面抗原はほかのウイルスであるため、中和活性の交差に関する解析に非常に重要である<sup>16)17)</sup>。

#### ● おわりに

HCV にはさまざまな実験系が開発された(表①)。ウイルスの培養系が利用できるようになりさらに HCV の生活環について詳細な検討が進み、新たな治療法の開発やワクチンの開発につながる事が期待されている。

#### 文 献

- 1) Choo QL *et al* : Isolation of a cDNA clone derived from a blood-borne non-A, non-B viral hepatitis genome. *Science* 244 : 359-362, 1989
- 2) Kolykhalov AA *et al* : Transmission of hepatitis C by intrahepatic inoculation with transcribed RNA. *Science* 277 : 570-574, 1997
- 3) Lohmann V *et al* : Replication of subgenomic hepatitis C virus RNAs in a hepatoma cell line. *Science* 285 : 110-113, 1999
- 4) Blight KJ *et al* : Efficient initiation of HCV RNA replication in cell culture. *Science* 290 : 1972-1974, 2000
- 5) Lohmann V *et al* : Mutations in hepatitis C virus RNAs conferring cell culture adaptation. *J Virol* 75 : 1437-1449, 2001
- 6) Blight KJ *et al* : Efficient replication of hepatitis C virus genotype 1a RNAs in cell culture. *J Virol* 77 :

- 3181-3190, 2003
- 7) Matsuura Y *et al* : Characterization of pseudotype VSV possessing HCV envelope proteins. *Virology* 286 : 263-275, 2001
  - 8) Bartosch B *et al* : Infectious hepatitis C virus pseudoparticles containing functional E1-E2 envelope protein complexes. *J Exp Med* 197 : 633-642, 2003
  - 9) Kato T *et al* : Sequence analysis of hepatitis C virus isolated from a fulminant hepatitis patient. *J Med Virol* 64 : 334-339, 2001
  - 10) Kato T *et al* : Efficient replication of the genotype 2a hepatitis C virus subgenomic replicon. *Gastroenterology* 125 : 1808-1817, 2003
  - 11) Date T *et al* : Genotype 2a hepatitis C virus subgenomic replicon can replicate in HepG2 and IMY-N9 cells. *J Biol Chem* 279 : 22371-22376, 2004
  - 12) Kato T *et al* : Nonhepatic cell lines HeLa and 293 support efficient replication of the hepatitis C virus genotype 2a subgenomic replicon. *J Virol* 79 : 592-596, 2005
  - 13) Wakita T *et al* : Production of infectious hepatitis C virus in tissue culture from a cloned viral genome. *Nat Med* 11 : 791-796, 2005
  - 14) Zhong J *et al* : Robust hepatitis C virus infection *in vitro*. *Proc Natl Acad Sci USA* 102 : 9294-9299, 2005
  - 15) Yi M *et al* : Production of infectious genotype 1a hepatitis C virus (Hutchinson strain) in cultured human hepatoma cells. *Proc Natl Acad Sci USA* 103 : 2310-2315, 2006
  - 16) Lindenbach BD *et al* : Complete replication of hepatitis C virus in cell culture. *Science* 309 : 623-626, 2005
  - 17) Pietschmann T *et al* : Construction and characterization of infectious intragenotypic and intergenotypic hepatitis C virus chimeras. *Proc Natl Acad Sci USA* 103 : 7408-7413, 2006

## HCVレプリコンシステム

国立感染症研究所ウイルス第二部・部長 脇田隆宇

ウイルス感染症に対する新たな治療法の開発や、ウイルスの基礎研究においてウイルス培養系による研究は不可欠である。しかし、HCVのウイルス培養がきわめて困難だったためHCVの研究は遅れてきた。HCVを培養細胞で増殖させる試みには、培養肝癌細胞、T細胞やB細胞などのリンパ球系細胞、初代培養肝細胞などが使用されてきたが、ウイルス複製は低いレベルでしかなく、多くは一過性の感染に終わった。非常に高感度なRT-PCR法を用いなければウイルスゲノムの検出は困難であり、HCVの感染複製の十分な解析は不可能だった。一方、多くのRNAウイルスでウイルスから精製したウイルスゲノムRNAあるいは試験管内で合成したRNAを培養細胞にトランスフェクションすることにより、ウイルスの複製増殖を観察できることが知られている。この方法によれば感染のステップを実験系から除外することができるので、ウイルス複製増殖をより多くの培養細胞で研究できる。しかし、チンパンジーの接種実験により感染性が確立されたHCVのcDNAクローンを用いてもHCVの培養細胞での複製増殖は観察できなかった。

しばらくの間、HCVのウイルス培養実験系開発には手詰まり感があったが、1999年にHCVレプリコンをBartenschlager博士（現ハイデルベルグ大学）のグループが初めて開発に成功した。HCVのウイルスゲノムの構造領域遺伝子を欠失させ、その部位に薬剤耐性遺伝子であるネオマイシン耐性遺伝子を挿入した。レプリコン構築を鋳型として試験管内でレプリコンRNAを合成して、その合成レプリコンRNAを導入したHuh7細胞をG418存在下に、2~4週間培養する。HCVレプリコンRNAが自律複製すると、ネオマイシン耐性遺伝子が発現し、細胞は生存することができ、コロニーを形成し増殖する。レプリコンが複製していない細胞はG418の作用により死滅する。また、コロニーを形成したレプリコン複製細胞をクローニングして増殖させることが可能である。レプリコン複製細胞ではHCV RNAが効率よく複製しており、複製しているRNAやウイルス蛋白質を容易に検出できる。この実験系を用いてNS3 プロテアーゼやNS5b ポリメラーゼ阻害薬が開発されてきている。レプリコンの欠点はウイルス粒子の産生が困難なことで、肝臓でのウイルスの感染複製をどの程度培養細胞レベルで再現しているかが検証困難な点である。しかし、HCVレプリコンは再現が容易な実験系であり、その研究は世界中に急速に普及している。

## NS3 プロテアーゼ・インヒビター

愛知医科大学消化器内科講師 奥村明彦  
愛知医科大学消化器内科教授 各務伸一

C型肝炎ウイルス（HCV）は宿主細胞内で1つのポリプロテインとして翻訳された後に、宿主あるいはHCV由来のシグナルペプチダーゼやプロテアーゼにより切断されて、core、envelopeなどの構造蛋白をはじめNS2、NS3、NS4A、NS4B、NS5A、NS5Bなどの非構造蛋白にプロセスされる。このうち、NS3のN末端側約3分の1に活性領域をもつNS3 プロテアーゼは、NS4からNS5に及ぶ大部分の非構造蛋白のプロセッシングに関与しているため、このNS3 プロテアーゼを標的としたプロテアーゼ・インヒビターの開発が進みつつある。現在、BILN-2061、VX-950、SCH503034の3つのNS3 プロテアーゼ・インヒビターが開発途上にある。



INSTITUT PASTEUR

Microbes and Infection xx (2007) 1–7



www.elsevier.com/locate/micinf

Original article

## GBV-B as a pleiotropic virus: distribution of GBV-B in extrahepatic tissues *in vivo*

Koji Ishii<sup>a</sup>, Sayuki Iijima<sup>b</sup>, Nobuyuki Kimura<sup>b</sup>, Young-Jung Lee<sup>b</sup>, Naohide Ageyama<sup>b</sup>, Shintaro Yagi<sup>d,1</sup>, Kenjiro Yamaguchi<sup>d</sup>, Noboru Maki<sup>d</sup>, Ken-ichi Mori<sup>d</sup>, Sayaka Yoshizaki<sup>a</sup>, Sanae Machida<sup>a,e</sup>, Tetsuro Suzuki<sup>a</sup>, Naoko Iwata<sup>c</sup>, Tetsutaro Sata<sup>c</sup>, Keiji Terao<sup>b</sup>, Tatsuo Miyamura<sup>a</sup>, Hirofumi Akari<sup>b,\*</sup>

<sup>a</sup> Department of Virology II, National Institute of Infectious Diseases, 1-23-1 Toyama, Shinjuku-ku, Tokyo 162-8640, Japan

<sup>b</sup> Laboratory of Disease Control, Tsukuba Primate Research Center, National Institute of Biomedical Innovation, 1-1 Hachimandai, Tsukuba, Ibaraki 305-0843, Japan

<sup>c</sup> Department of Pathology, National Institute of Infectious Diseases, 1-23-1 Toyama, Shinjuku-ku, Tokyo 162-8640, Japan

<sup>d</sup> Advanced Life Science Institute, Wako, Saitama 351-0112, Japan

<sup>e</sup> Department of Microbiology, Saitama Medical School, Moroyama-Cho, Iruma-Gun, Saitama 350-0495, Japan

Received 25 August 2006; accepted 16 January 2007

### Abstract

GB virus B (GBV-B) infection of New World monkeys is considered to be a useful surrogate model for hepatitis C virus (HCV) infection. GBV-B replicates in the liver and induces acute resolving hepatitis but little is known whether the other organs could be permissive for the virus. We investigated the viral tropism of GBV-B in tamarins in the acute stage of viral infection and found that the viral genomic RNA could be detected in a variety of tissues. Notably, a GBV-B-infected tamarin with marked acute viremia scarcely showed a sign of hepatitis, due to preferential infection in lymphoid tissues such as lymph nodes and spleen. These results indicate that GBV-B as well as HCV is a pleiotropic virus *in vivo*. © 2007 Elsevier Masson SAS. All rights reserved.

**Keywords:** GB virus B; Hepatitis C virus; Tamarin; Surrogate model

### 1. Introduction

Over 100 million people worldwide are carriers of hepatitis C virus (HCV) and the viral infection is a significant cause of human morbidity and mortality; chronic HCV infection in many cases will lead to liver cirrhosis and hepatocellular carcinoma. Furthermore, HCV infection manifests a variety of extrahepatic, at least in part due to the extrahepatic tropisms of HCV, particularly lymphotropism diseases (for review see [1]).

Other than humans, only chimpanzees that are endangered as species can be productively infected by HCV. Together with ethical issues regarding animal experiments, it has become increasingly difficult to access chimpanzees for experimental studies. Tamarins (*Saguinus* species), one of the new world monkeys, develop acute, self-limited hepatitis upon infection with the GB virus B (GBV-B), which is most closely related to HCV [2–4]. Although the acute nature of GBV-B infection in tamarins has been distinguished this hepatitis from HCV infection in humans, recent studies demonstrated that tamarins could be persistently infected by GBV-B and developed chronic hepatitis [5,6]. Therefore, the GBV-B infection of tamarins is proposed as a good surrogate model for hepatitis C. While GBV-B appeared to infect liver, comprehensive documentation of the *in vivo* tropism of GBV-B has not been

\* Corresponding author. Tel.: +81 29 837 2121; fax: +81 29 837 0218.

E-mail address: akari@nibio.go.jp (H. Akari).

<sup>1</sup> Present address: Laboratory of Cellular Biochemistry, Department of Animal Resource Sciences, Graduate School of Agricultural and Life Sciences, The University of Tokyo, Tokyo, Japan.

reported yet. A previous report that GBV-B RNA was observed in peripheral blood mononuclear cells (PBMCs) from a GBV-B-infected marmoset [7] suggests that GBV-B may be lymphotropic as well as HCV. Considering the close similarity between HCV and GBV-B, we examined the viral distribution and tropism in tamarins in the acute phase of the viral infection.

## 2. Materials and methods

### 2.1. Animals

Adult white-lipped and Red-handed tamarins (*Saguinus labiatus* and *Saguinus midas*, respectively) were housed in individual cages at the Tsukuba Primate Research Center. All animal studies were conducted in accordance with the protocols of experimental procedures that were approved by the Animal Welfare and Animal Care Committees of the National Institute of Biomedical Innovation and National Institute of Infectious Diseases. The details of tamarins used in this study were summarized in Table 1.

### 2.2. GBV-B infection in tamarins

GBV-B RNA was transcribed *in vitro* with T7 RNA polymerase (Promega, Madison, WI) from 10 µg of *Xho*I-digested pGBB [2] that harbors infectious cDNA for GBV-B (kind gift of Dr. J. Bukh, National Institutes of Health, USA). The integrity of the RNA was checked by electrophoresis through an agarose gel stained with ethidium bromide. Each transcription mixture (400 µg of GBV-B RNA) was diluted with 400 µl of ice-cold water and then immediately frozen on dry ice and stored at –80 °C. Transcription mixtures were injected into

each tamarin intrahepatically. For transmission of GBV-B, animals were infected intrahepatically with 100 µl of GBV-B infectious plasma containing  $8 \times 10^8$  genome equivalents (GE) of the viral RNA. Blood samples were periodically collected from the monkeys from femoral vein under anesthetization and were tested for plasma ALT level.

### 2.3. Quantification of GBV-B genomic RNA

GBV-B-infected tamarins were euthanized and perfused with saline thoroughly before the collection of specimens including plasma, PBMCs and a variety of tissues (esophagus, stomach, duodenum, jejunum, ileum, cecum, colon, rectum, liver, pancreas, submandibular gland, trachea, lung, bone marrow, thymus, spleen, submandibular lymph nodes, axillary lymph nodes, intestinal lymph nodes, mesenteric lymph nodes, inguinal lymph nodes, tonsil, heart, kidney, adrenal gland, bladder, brain, spinal cord, testis, uterus and ovary). GBV-B RNA from these specimens was quantified by a real-time, 5' exonuclease PCR (TaqMan) assay using a primer-probe combination that recognized a portion of the GBV-B capsid gene. The primers 558F [5' AACGAGCAAAGCGCAAAGTC] and 626R [5' CATCATGGATAACCAGCAATTTTGT] and probe 579P [5' 6FAM-AGCGCGATGCTCGGCCTCGTATAMRA] [8] were obtained from PE Biosystems. The primers were used at 15 pmol/50 µl reaction, and the probe was used at 10 pmol/50 µl reaction. Synthesized GBV-B RNA was used as a reference standard of GBV-positive plasma. PBMCs were isolated from whole blood by density-gradient centrifugation. Approximately 10 mg of tissues were removed under sterile conditions and immediately homogenized in 1 ml of TRIzol (Invitrogen, Carlsbad, CA) to extract RNA. We set our lowest detection cutoff at  $10^2$  GE per ml. All the specimens were evaluated in duplicates and the averages were shown.

Table 1  
Summary of the results of GBV-B RNA levels in the tissues of the virus-infected tamarins

		Tm3	Tm4	Tm5	Tm6
Animals		<i>S. labiatus</i>	<i>S. midas</i>	<i>S. labiatus</i>	<i>S. midas</i>
Sex		Female	Female	Male	Female
GBV-B inoculum		Plasma	Plasma	RNA	RNA
Weeks at necropsy		4	4	3	ND <sup>a</sup>
ALT		321	522	38	554
Viral loads in:					
Blood	Plasma	$3.8 \times 10^8$	$5.9 \times 10^8$	$1.3 \times 10^{10}$	$2.8 \times 10^9$
	PBMC	270	1630	35650	ND
Spleen		(–) <sup>b</sup>	540	5980	ND
Lymph nodes	Inguinal	(–)	(–)	3090	ND
	Intestinal	(–)	(–)	640	ND
Liver		70080	33480	16080	ND
Kidney		(–)	(–)	380	ND
Testis				600	ND
Ovary		1290	150		ND
Bone marrow		120	(–)	750	ND

Viral loads in each tissues were presented as GE/mg except for plasma (GE/ml) and PBMC (GE/ $10^6$  cells). Data for Tm6 were obtained at week 4.

<sup>a</sup> ND: not done.

<sup>b</sup> (–): undetectable.

Please cite this article in press as: K. Ishii et al., GBV-B as a pleiotropic virus: distribution of GBV-B in extrahepatic tissues *in vivo*, *Microb Infect* (2007), doi:10.1016/j.micinf.2007.01.010



#### 2.4. Detection of anti-GBV-B core and NS3 antibodies by ELISA

The TrpE-core (aa 1 to 132) fusion protein and TrpE-NS3 (aa 1135 to 1378) fusion protein, representing a portion of NS3 identified as being immunogenic in infected animals [9], was expressed in *Escherichia coli* [10] to serve as an antigen to generate polyclonal rabbit antisera. Tamarin sera were tested for the presence of antibodies to GBV-B core and NS3 by ELISA as described previously [8].

#### 2.5. Cloning of entire GBV-B genome from plasma, liver and PBMCs of infected tamarins

GBV-B RNA was isolated from plasma, liver and PBMCs as described above. GBV-B cDNA was synthesized using SuperScript reverse transcriptase II (Invitrogen) with GB-5145R primer (5'-GCG AGT GCG GCT GTC CCA GAA GTA TTG ACT-3') or GB-9051R primer (5'-AAT TTG GGG GTT CAG CTG ATG GCT AAT CCA-3'). After RNase H (Invitrogen) treatment at 42 °C, a cDNA mixture was subjected to PCR with LA-taq DNA polymerase (TaKaRa), GB-5145R primer and GB-35S primer (5'-ACC ACA AAC ACT CCA GTT TGT TAC ACT CCG CTA GG-3') or GB-9051R primer and GB-3999S primer (5'-CGT ACG GCG TGA ATC CAA ATT GCT ATT TTA-3') for 30 cycles of denaturation at 94 °C for 20 s and extension at 68 °C for 5 min. PCR products were purified from the gel using a QIA-quick gel kit (Qiagen), and then cloned into pGEM-T Easy vector (Promega). Four clones of each fragment were determined using a CEQ-2000XL analysis system with a DTCS quick start kit and GBV-B specific primers according to the manufacturer's instructions. Sequence data were analyzed on Macintosh computers with the Sequencer (Gene Code Corp.) and MacVector (Accelrys) software packages.

#### 2.6. Synthesis of positive and negative standard RNAs for RT-PCR controls

Recombinant positive and negative strand RNAs were generated from pGBB containing 3' sequences of GBV-B. Positions 8569–9359 were amplified and inserted into pGEM-T easy vector. Clones were selected for sense and antisense orientation of the insert corresponding to positive and negative strands, respectively. Ten micrograms of the selected plasmids were linearized using *Pst*I and positive- and negative-strand RNAs were synthesized by transcription from the upstream T7 RNA polymerase promoter by Ambion MEGAscript T7 kit (Ambion, Austin, TX).

#### 2.7. Detection of strand-specific viral RNA by tagging PCR system

One microgram of total RNA obtained from tissues or cells was subjected to RT-PCR. cDNAs were synthesized using Superscript III first strand synthesis system (Invitrogen). In order to overcome the detection of falsely primed cDNA products and make the PCR system strand-specific, additional

nucleotides (TCATGGTGGCGAATAA) were added to the 5' end of the reverse transcription primer (5'-TCATGGTGGCGAATAATTGGATTAGCCATCAGCTGAACC-3'), forming a "tag" (underlined) [11,12]. This "tag" sequence was neither complementary nor homologous to any part of the GBV-B genome. PCR amplification of a tagged cDNA was performed using only the tag portion of the cDNA primer (5'-TCATGGTGGCGAATAA-3') as one of the primers and a GBV-B specific oligonucleotide for the opposing primer (5'-CTTGGTACTACGCTCTGCACA-3', positions 9339–9359). For the first round of PCR using 2 µl of cDNA in a final volume of 25 µl, the reactions were performed using a TaKaRa PCR kit (TaKaRa) with following conditions; a 20 s and 94 °C denaturation step followed by 20 s and 55 °C annealing and 2 min and 72 °C extension steps. After 30 cycles of first round amplification, 2 µl of reaction samples were subjected to 30 cycles of nested PCR using 5'-TTTAGGGCAGCGGCAACAG-3' (positions 9105–9124) and 5'-CACACAGCCAGGACTCCTCA-3' (positions 9260–9279) as primers.

#### 2.8. Histopathology

Five tamarin livers were used in this study. Of these, three livers were from GBV-B-infected tamarins (Table 1), and two were from uninfected tamarins. Liver samples obtained by necropsy were fixed with 4% paraformaldehyde, embedded in paraffin, and cut into 4 µm thick-sections. Deparaffinized sections were stained with hematoxylin and eosin (H&E) for histopathological analyses. To investigate apoptotic cells in the livers, we also examined both DNA fragmentation and immunohistochemistry for an active form of caspase-3. To diminish autofluorescence mainly caused by lipofuscin, sections were pre-stained with 1% Sudan black B. DNA fragmentation was evaluated by a TUNEL assay with an ApopTag Direct *In Situ* Apoptosis Detection Kit (Chemicon International, Temecula, CA) according to the manufacturer's instructions. Briefly, the specimens were digested with a solution of proteinase K (20 µg/ml) in PBS for 5 min and then incubated with terminal deoxynucleotidyl transferase (TdT) and fluorescein-labeled nucleotides (ApopTag Direct) in a humid atmosphere at 37 °C for 1 h. Specimens were viewed with a BX-FLA fluorescence microscope (Olympus, Tokyo, Japan). To control for nonspecific incorporation of nucleotides and nonspecific binding of TdT, cells were treated with proteinase K as usual, but staining was performed in the absence of active TdT. This served as a negative control. In parallel, immunohistochemistry for an active form of caspase-3 was examined by using an FITC-conjugated monoclonal antibody against the active caspase-3 (C92-605; BD Pharmingen, San Jose, CA) in order to confirm the degree of apoptotic cells detected by TUNEL staining. Sections were deparaffinized followed by autoclaving for 5 min at 121 °C, and then incubated free floating in the primary antibody solution overnight at 4 °C. Following brief washes, sections were then incubated with DAPI (1:800; Santa Cruz Biotechnology, Santa Cruz, CA) for 1 h at room temperature. These sections were examined with a Digital Eclipse C1 confocal microscope (Nikon, Japan).

### 3. Results

#### 3.1. GBV-B infection in tamarins

Firstly, two tamarins were intrahepatically inoculated with RNA transcripts from GBV-B infectious molecular clone pGBB (Fig. 1). Both monkeys showed viremia at 2 weeks post inoculation; peak viral titers in plasma reached up to  $10^9$  GE/ml and both monkeys developed hepatitis with dramatically elevated plasma ALT levels. The viremia was maintained up to 8 weeks, followed by rapid decline in parallel with the resolution of the ALT abnormalities. Within 6–8 weeks of the inoculation, the development of antibodies reactive with the viral core and NS3 proteins was observed (Fig. 1). Multiple plasma samples collected at later time points contained no detectable viral RNA and showed no ALT abnormalities; however, antibodies against GBV-B core and NS3 proteins were maintained at relatively high levels at least until 28 weeks after inoculation (Fig. 1). These results confirmed that inoculation of GBV-B viral RNA caused acute hepatitis in parallel with typical viremia in tamarins.

Next, in order to examine the tissue tropism of GBV-B *in vivo*, four tamarins were inoculated intrahepatically with week 2 plasma of tamarin Tm1 containing  $8 \times 10^8$  GE of GBV-B (Tm3 and Tm4) or synthetic GBV-B RNA as described above (Tm5 and Tm6). These tamarins developed a typical acute infection that were marked by high levels of viremia, indicating that inoculation of either viral RNA or plasma of the infected tamarin resulted in comparable outcome (Fig. 2). It is noteworthy that in Tm5 the plasma ALT level was scarcely elevated in contrast with other three tamarins during the acute period of GBV-B infection, although this tamarin developed highest viremia ( $1.3 \times 10^{10}$  GE/ml).

#### 3.2. Histopathological analyses of GBV-B infection

Histopathological analyses in Tm3 and Tm4 livers showed inflammatory responses including inflammatory cell invasions around central and/or portal veins and hemorrhages, hepatocytic degenerations, and disruptions of sinusoids (Fig. 3A,B,E,F). Although there were only minimal pathological changes, hepatocytic degenerations and dilation of sinusoids were also found in the Tm5 liver (Fig. 3C and G) in contrast to uninfected tamarins (Fig. 3D and H, data not shown). To further evaluate the levels of apoptotic hepatocytes in these monkeys, we employed two different methods, detecting fragmented DNA (TUNEL assay) and an active form of caspase-3 as previously described [13]. It was found that substantial numbers of fragmented DNA-positive cells were observed in the Tm3 and Tm4 livers while much less in the Tm5 liver (Fig. 3I–K). Consistent results were obtained when the active form of caspase-3 was stained (Fig. 3M–O). On the other hand, we found neither DNA fragmentation nor caspase-3 activation in uninfected tamarin livers (Fig. 3L and P, data not shown). The minimal levels of pathological changes in the Tm5 liver were well correlated with a lower level of plasma ALT in Tm5 (Fig. 2, Table 1).

#### 3.3. Tissue distribution of GBV-B

The results described above suggested the possibility that the substantial levels of viral replication occurred in other tissues rather than in the liver of Tm5. To ascertain the possibility, we euthanized three tamarins (Tm3, Tm4 and Tm5) and the viral levels in a variety of tissues were compared. Table 1 summarizes the data obtained in this experiment. It is reasonable to consider that GBV-B replicated in the liver accounts for majority of the viral load *in vivo*. However,

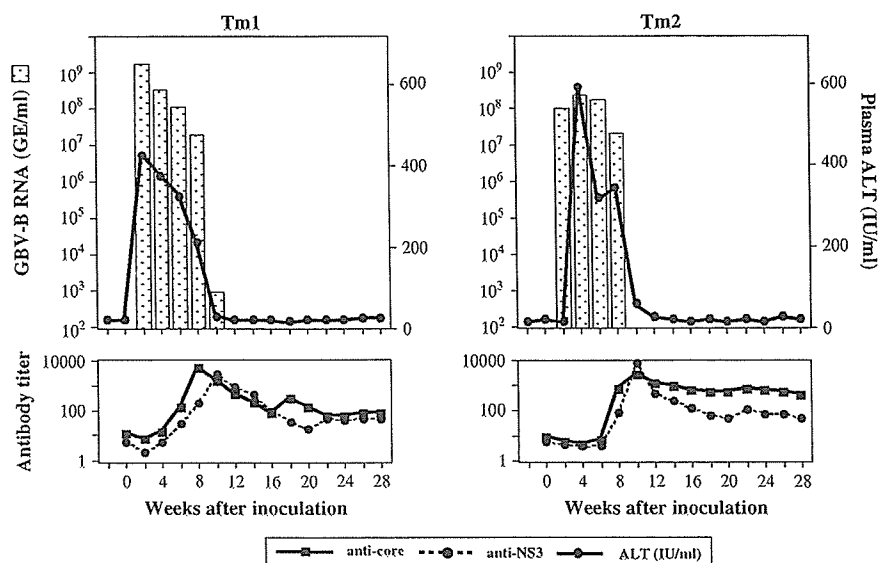


Fig. 1. Course of GBV-B infection in tamarins Tm1 and Tm2. Synthesized infectious RNA transcript of GBV-B from a pGBB molecular clone was inoculated into each tamarin intrahepatically. Plasma samples were collected from each tamarin at 2-week intervals post inoculation. The viral RNA copies, ALT levels, and titers of anti-viral antibodies (anti-core and anti-NS3) in the plasma samples until 28 weeks after inoculation were shown.

substantial levels of GBV-B RNA were detected not only in the liver but also in a variety of extrahepatic tissues such as hemolymphoid and genital tissues, suggesting that GBV-B may infect and replicate in these organs. Notably, the viral RNA levels of Tm5 were much greater in the lymphoid tissues but lower in the liver as compared with those of other two tamarins, indicating that the highest plasma viral load in Tm5 derived from extrahepatic tissues, mainly hemolymphoid tissues. We could not detect GBV-B RNA from other tissues tested (data not shown). From these results, we concluded that the preferential distribution of GBV-B in the extrahepatic tissues rather than in the liver of Tm5 may attribute to the highest plasma viral load in spite of the mild disorder and the lower viral load in the liver.

In addition, the unique viral distribution implied that the GBV-B disseminated in Tm5 might acquire novel tissue tropism as a result of genomic mutation. To ascertain the possibility, we amplified the entire viral genomes by RT-PCR from the liver, PBMCs and plasma collected from Tm5 at euthanasia and compared with the original nucleotide sequence. The sequences determined were completely identical to the original sequence of GBV-B (data not shown), indicating that the sequence heterogeneity of GBV-B was not responsible for the different tropism observed in Tm5 and thus GBV-B intrinsically exhibits pleiotropism in a host-dependent manner.

#### 3.4. Detection of strand-specific viral RNA in the tamarin tissues

To confirm that the virus was actually replicated in the tissues other than the liver, we sought to differentially determine negative-strand viral RNA which is shown to be a viral replication intermediate in case of HCV. We thus newly developed an assay system for detecting replication intermediate of GBV-B.

To determine the sensitivity of this method, synthetic positive- and negative-strand GBV-B transcripts (ranging from  $10^8$  to  $10^0$  copies of GBV-B) in 100-fold serial dilutions were subjected to RT-PCR. As shown in Fig. 4A, at least 100 copies of GBV-B negative-strand RNA could be detected by this method. When the primer for cDNA synthesis was omitted, no PCR products were obtained (Fig. 4A, negative control), indicating that the PCR signals were derived specifically from the GBV-B negative-strand RNA. In the presence of  $10^8$  copies of positive-strand HCV RNA, false positive PCR signals appeared (Fig. 4A). We then analyzed the samples from liver, spleen, pancreas, stomach and PBMCs from Tm5 using the GBV-B strand-specific PCR assay and found that the negative-strand viral RNAs were detected in the liver, spleen and PBMC samples (Fig. 4B). No negative-strand or replicating forms of the virus were detected from RNA extracted from pancreas, stomach and HeLa cells.

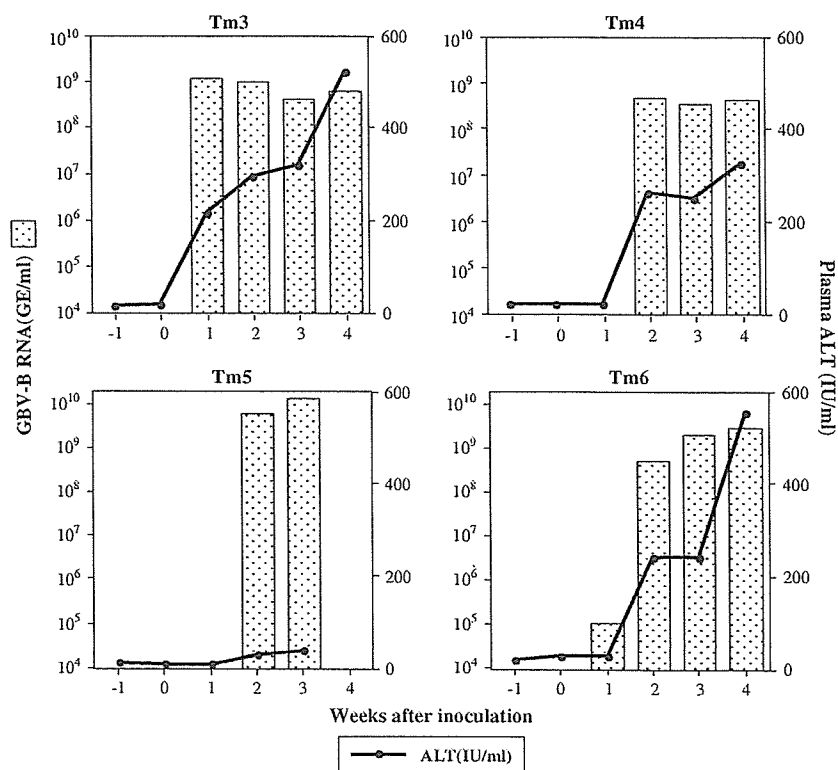


Fig. 2. Acute course of GBV-B infection in tamarins (Tm3 and Tm4) by *in vivo* passage of plasma ( $7.9 \times 10^8$  GE/head) obtained from the GBV-B RNA-inoculated Tm1 in comparison with GBV-B RNA transcript-inoculated tamarins (Tm5 and Tm6). The viral RNA copies and ALT levels in the plasma samples collected from each tamarin were indicated.

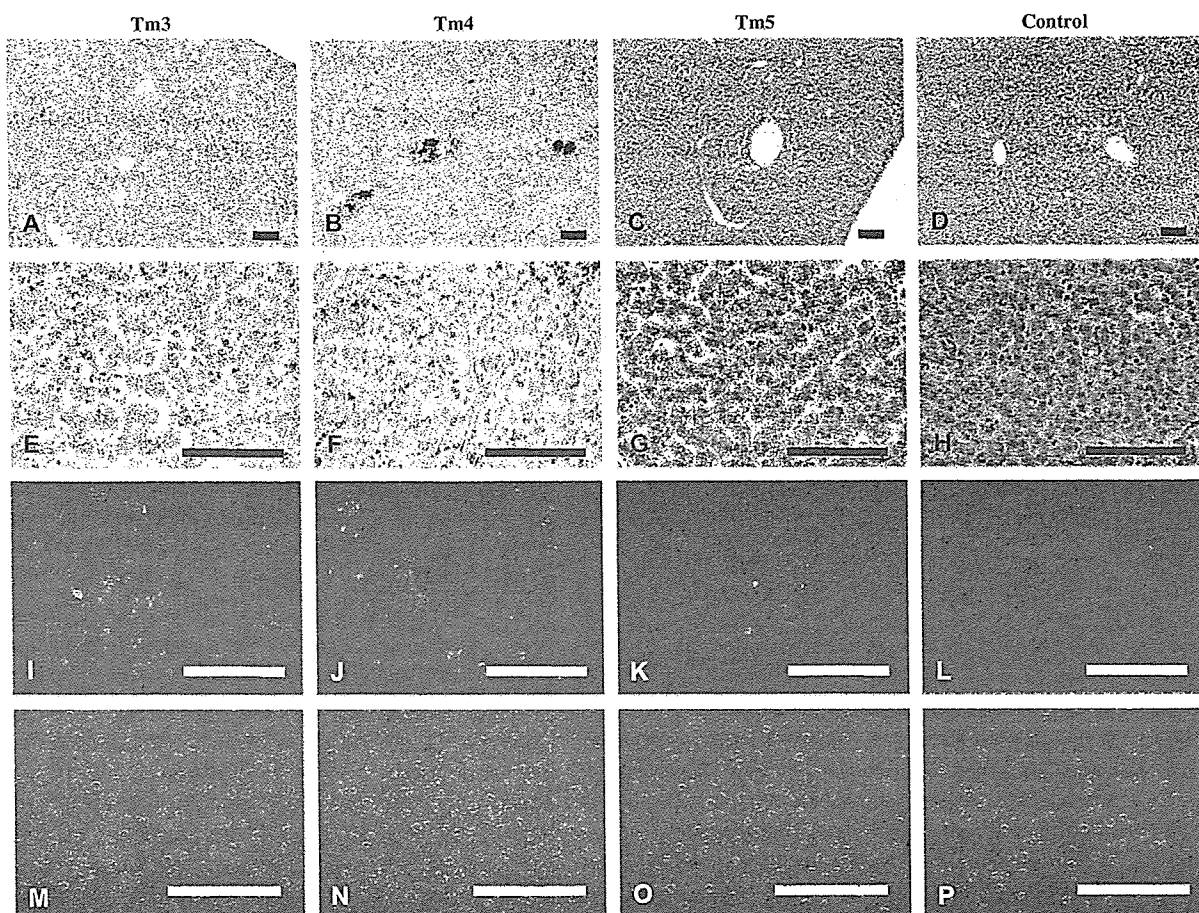


Fig. 3. Photomicrographs of liver sections from Tm3 (A, E, I, M), Tm4 (B, F, J, N), Tm5 (C, G, K, O), and an uninfected tamarin (D, H, L, P). A–H show sections with H&E staining, while I–L and M–P indicate sections with a TUNEL assay and immunohistochemistry for an active form of caspase-3, respectively. Sections immunostained for an active form of caspase-3 (green fluorescent) were counterstained with DAPI (blue fluorescent). Scale bars: 100  $\mu$ m.

#### 4. Discussion

GBV-B is most closely related to HCV and induces acute resolving hepatitis in tamarins. It is therefore reasonable that GBV-B has been considered to be a hepatotropic virus; in this study, however, we show for the first time that GBV-B is a pleiotropic virus and can disseminate to not only liver but also a variety of extrahepatic tissues such as hemolymphoid and genital tissues. Of note, there is ample evidence that persistent HCV infection manifests a variety of extrahepatic diseases, at least in part due to the extrahepatic tropisms of HCV (for review see [1]). This also suggests that extrahepatic tissues may serve as alternative reservoirs for HCV, while further analyses should still be required to understand the viral dynamics *in vivo*. Considering the similar pleiotropism of HCV and GBV-B, our results support and extend the usefulness of New World primates infected with GBV-B as a surrogate model for the study of pathogenesis and tropism of HCV infection.

Tamarins infected with GBV-B generally develop semi-acute viremia, of which peak levels regularly ranged from  $10^7$  to  $10^9$  GE/ml on the basis of previous reports [2,5,6,

14,15]. From this point of view, the peak viremia ( $1.3 \times 10^{10}$  GE/ml) in Tm5 euthanized at the acute phase of the viral infection appeared to be much greater than other cases. It seems likely that in Tm5 the lymphoid tissues but not liver were responsible for the highly efficient viral production, because (i)

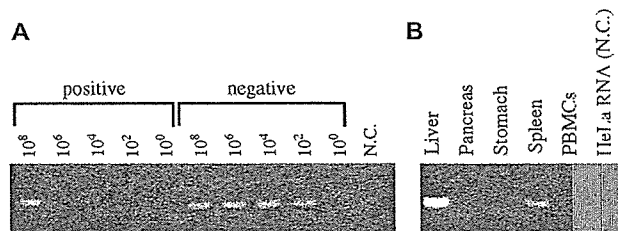


Fig. 4. (A) Titration of synthetic GBV-B RNA transcripts. Synthetic RNA transcripts corresponding to the positive- and negative-strands of part of the GBV-B were serially diluted and each transcript was subjected to amplification using strand-specific RT-PCR to determine the specificity and sensitivity of the assays. (B) Detection of negative-strand GBV-B RNA from various tissues. One microgram of total RNA obtained from tissues or cells was subjected to RT-PCR.

viral titer in the liver was lowest among three monkeys, which was consistent with minimal plasma ALT level and liver damage; (ii) yet, Tm5 exhibited highest viremia levels, (iii) the viral RNA levels in PBMCs, spleen and inguinal and intestinal lymph nodes of Tm5 were much greater than others, and (iv) we could detect negative-strand GBV-B RNA from not only liver but also spleen and PBMCs. Supposing that the entire virus in Tm3 plasma ( $3.8 \times 10^8$  GE/ml) was produced in the liver of which RNA titer was highest among tamarins, most of the virus in Tm5 plasma ( $1.3 \times 10^{10}$  GE/ml) should be derived from extrahepatic tissues. Taken together, our data demonstrate preferential dissemination of GBV-B in extrahepatic tissues. In order to further define the cell type(s) in which GBV-B replicates efficiently, *in situ* histological analysis should be needed as indicated in the case of HCV [16].

It was possible that differential lymphotropism among GBV-B-infected tamarins could be due to adaptive mutation in the viral genome. From this point of view, we cloned the viral RNA obtained from plasma and liver; however, we did not find any sequence heterogeneity in the viral genome (data not shown). Furthermore, challenge of Tm5 plasma to naïve tamarins developed typical semi-acute hepatitis with regular viremia and did not reproduce the preferential lymphotropism (data not shown). These results indicate that GBV-B intrinsically has pleiotropism in a host-dependent manner. It is possible that multiple surface molecules in the host cells, which act as alternative receptors, would determine the pleiotropism of GBV-B. It remains to be investigated whether host molecules which are used as receptors for HCV [17] would also be used by GBV-B.

Histopathological studies showed the inflammatory responses in Tm3 and Tm4 livers; especially, the Tm4 liver developed strong degenerative changes, which was consistent with high ALT levels (Fig. 2G,H). Furthermore, the livers of Tm3 and Tm4 showed substantial proportions of apoptotic cells as revealed by greater signals of DNA fragmentation and caspase-3 activation, both of which were popular markers of apoptosis, than those in Tm5 (Fig. 3). It needs to be clarified whether such cytopathic effects could be directly induced by GBV-B infection into hepatocytes or whether effector cytotoxic T lymphocytes would be responsible for the cytopathicity.

#### Acknowledgments

We are grateful to Dr. Jens Bukh for providing pGGB. We also thank Mami Matsuda, Makiko Yahata and Tetsu Shimoji for technical assistance and members of Corporation for Production and Research of Laboratory Primates for the handling and care of the monkeys. This work was supported by a Health and Labour Science Research Grant from the Ministry of Health, Labour, and Welfare, Japan, and from New

Energy and Industrial Technology Development Organization (NEDO) of Japan.

#### References

- [1] V. Agnello, F.G. De Rosa, Extrahepatic disease manifestations of HCV infection, *J. Hepatol.* 40 (2004) 341–352.
- [2] J. Bukh, C.L. Apgar, M. Yanagi, Toward a surrogate model for hepatitis C virus: An infectious molecular clone of the GB virus-B hepatitis agent, *Virology* 262 (1999) 470–478.
- [3] A.S. Muerhoff, et al., Genomic organization of GB viruses A and B: two members of the Flaviviridae associated with GB agent hepatitis, *J. Virol.* 69 (1996) 5621–5630.
- [4] J.N. Simons, et al., Identification of two flavivirus-like genomes in the GB hepatitis agent, *Proc. Natl. Acad. Sci. USA.* 92 (1995) 3401–3405.
- [5] A. Martin, F. Bodola, D.V. Sangar, K. Goettge, V. Popov, R. Rijnbrand, R.E. Lanford, S.M. Lemon, Chronic hepatitis associated with GB virus B persistence in a tamarin after intrahepatic inoculation of synthetic viral RNA, *Proc. Natl. Acad. Sci. USA.* 100 (2003) 9962–9967.
- [6] J.H. Nam, K. Faulk, R.E. Engle, S. Govindarajan, M. St Claire, J. Bukh, In vivo analysis of the 3' untranslated region of GB virus B after *in vitro* mutagenesis of an infectious cDNA clone: persistent infection in a trans-fected tamarin, *J. Virol.* 78 (2004) 9389–9399.
- [7] J.R. Jacob, K.C. Lin, B.C. Tennant, K.G. Mansfield, GB virus B infection of the common marmoset (*Callithrix jacchus*) and associated liver pathology, *J. Gen. Virol.* 85 (2004) 2525–2533.
- [8] B. Beames, D. Chavez, B. Guerra, L. Notvall, K.M. Brasky, R.E. Lanford, Development of a primary tamarin hepatocyte culture system for GB virus-B: a surrogate model for hepatitis C virus, *J. Virol.* 74 (2000) 11764–11772.
- [9] T.J. Pilot-Matias, A.S. Muerhoff, J.N. Simons, T.P. Leary, S.L. Buijk, M.L. Chalmers, J.C. Erker, G.J. Dawson, S.M. Desai, I.K. Mushahwar, Identification of antigenic regions in the GB hepatitis viruses GBV-A, GBV-B, and GBV-C, *J. Med. Virol.* 48 (1996) 329–338.
- [10] K. Tsukiyama-Kohara, N. Iizuka, M. Kohara, A. Nomoto, Internal ribosome entry site within hepatitis C virus RNA, *J. Virol.* 66 (1992) 1476–1483.
- [11] R.L. Chaves, J. Graff, A. Normann, B. Flehmig, Specific detection of minus strand hepatitis A virus RNA by Tail-PCR following reverse transcription, *Nucleic Acids Res.* 22 (1994) 1919–1920.
- [12] J. Mellor, G. Haydon, C. Blair, W. Livingstone, P. and Simmonds, Low level or absent *in vivo* replication of hepatitis C virus and hepatitis G virus/GB virus C in peripheral blood mononuclear cells, *J. Gen. Virol.* 79 (1998) 705–714.
- [13] H. Akari, S. Bour, S. Kao, A. Adachi, K. Strebel, The human immunodeficiency virus type 1 accessory protein Vpu induces apoptosis by suppressing the nuclear factor kappaB-dependent expression of antiapoptotic factors, *J. Exp. Med.* 194 (2001) 1299–1311.
- [14] A. Sbardellati, E. Scarselli, E. Verschoor, A. De Tomassi, D. Lazzaro, C. Traboni, Generation of infectious and transmissible virions from a GB virus B full-length consensus clone in tamarins, *J. Gen. Virol.* 82 (2001) 2437–2448.
- [15] R.E. Lanford, D. Chavez, L. Notvall, K.M. Brasky, Comparison of tamarins and marmosets as hosts for GBV-B infections and the effect of immunosuppression on duration of viremia, *Virology* 311 (2003) 72–80.
- [16] E.J. Gowans, Distribution of markers of hepatitis C virus infection throughout the body, *Semin. Liver Dis.* 20 (2000) 85–102.
- [17] L. Cocquerel, C. Voisset, J. Dubuisson, Hepatitis C virus entry: potential receptors and their biological functions, *J. Gen. Virol.* 87 (2006) 1075–1084.

# Rapid Genome Sequencing of RNA Viruses

Tetsuya Mizutani,\* Daiji Endoh,†  
 Michiko Okamoto,‡ Kazuya Shirato,\*  
 Hiroyuki Shimizu,\* Minetaro Arita,\*  
 Shuetsu Fukushi,\* Masayuki Saijo,\*  
 Kouji, Sakai,\* Chang Kweng Lim,\* Mikako Ito,\*  
 Reiko Nerome,\* Tomohiko Takasaki,\* Koji Ishii,\*  
 Tetsuro Suzuki,\* Ichiro Kurane,\*  
 Shigeru Morikawa,\* and Hidekazu Nishimura‡

We developed a system for rapid determination of viral RNA sequences whereby genomic sequence is obtained from cultured virus isolates without subcloning into plasmid vectors. This method affords new opportunities to address the challenges of unknown or untypeable emerging viruses.

Over the past few years, global migration has led to emerging infectious diseases that pose substantial risks to public health. To prevent potential outbreaks, early detection of infectious pathogens is necessary. In particular, the recent outbreak of severe acute respiratory syndrome (SARS) provided important lessons on how unknown viruses should be detected rapidly. Thus, a standardized and qualified system is required for rapid nucleic acid sequence determination for newly emerging viruses.

Recently, we developed a new method for detecting RNA viruses. This method, based on cDNA representational difference analysis (cDNA RDA), uses 96 hexanucleotides that are not suitable for priming ribosomal RNAs but that normally prime most of the genome of an RNA virus as primers for reverse transcription in cDNA RDA (1). However, the RDA method with a cloning step requires at least 1 week for the determination of the nucleic acid sequence.

## The Method

Our new system for rapid determination of viral RNA sequence (RDV) uses whole-genome amplification and direct sequencing techniques (Figure 1). The RDV method comprises 6 procedures: 1) effective destruction of cellular RNA and DNA for semipurification of viral particles, 2) effective elimination of DNA fragments by using a pre-

filtration column system and elution of small amounts of RNA, 3) effective synthesis of first- and second-strand cDNAs, 4) construction and amplification of a cDNA library, 5) construction of a second cDNA library, and 6) direct sequencing using optimized primers. The RDV method enables a broad range of partial nucleotide sequences within the entire viral RNA genome to be obtained within 2 days without cloning into plasmids.

To eliminate contaminating cellular RNA and DNA from the samples, 0.001 µg of RNase A (Qiagen, Hilden, Germany) and 1 µL (2 U) of Turbo DNA-free DNase I (Ambion, Austin, TX, USA) with 1× Turbo DNA-free buffer were incubated at 37°C for 30 min under conditions that prevented destruction of viral RNA in the viral particles. The RNA in the viral particles was then extracted within 30 min by using a total RNA isolation mini kit (Agilent Technologies Inc., Palo Alto, CA, USA). We confirmed that DNA was effectively eliminated by this RNA extraction kit.

In accordance with the Invitrogen manual, cDNA was synthesized, by using random hexamers (Takara Bio Inc., Kyoto, Japan) and Superscript III (Invitrogen, Carlsbad, CA, USA) lacking RNase H activity, at 50°C for 1 h. Then 60 U of RNase H (Takara Bio Inc.) added before synthesis of second-strand cDNA at 50°C for 1 h. In accordance with the manual, a whole genome amplification system (WGA; Sigma-Aldrich, Saint Louis, MO, USA), which was developed for amplification of genomic DNA, was used to amplify viral double-stranded cDNA. This process was

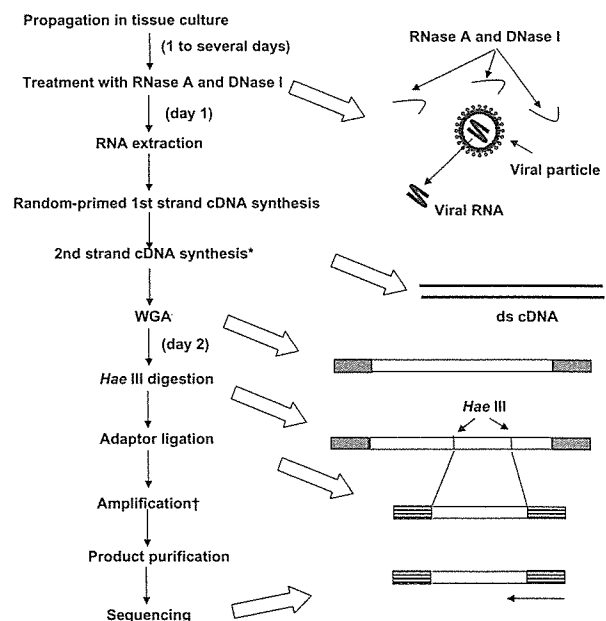


Figure 1. Overall scheme of the rapid determination of viral RNA sequence method. \*By adding RNase H; WGA, whole genome amplification; †With specially designed primer sets as shown in Figure 2.

\*National Institute of Infectious Diseases, Tokyo, Japan; †Rakuno Gakuen University, Ebetsu, Japan; and ‡Sendai Medical Center, Sendai, Japan

performed within 90 min. Instead of the Taq polymerase recommended in the kit, we used 1.25 U of AmpliTaq Gold LD (Applied Biosystems, Foster City, CA, USA) to obtain a high yield of the PCR products. Primers were provided in the WGA kit, but no information regarding their sequences was obtained. The reaction mixture was heated at 95°C for 9 min (for activation of AmpliTaq Gold), followed by 70 cycles of amplification using Mastercycler (Eppendorf AG, Hamburg, Germany). Each PCR cycle consisted of annealing at 68°C for 1 min, primer extension at 72°C for 5 min, and denaturation at 94°C for 1 min.

The 1st cDNA library was digested with 40 U of *Hae*III (Takara Bio Inc.) at 37°C for 30 min. DNA was purified by using the MonoFas DNA isolation system (GL Science, Tokyo, Japan), and a blunt *Eco*RI-*Not*I-*Bam*HI adaptor (10 pmol; Takara Bio Inc.) was ligated at 16°C for 30 min by using DNA Ligation Kit, Mighty Mix (Takara Bio Inc.). The second cDNA library was amplified by PCR with specially designed primer sets in which 6 nucleotides composed of CC (*Hae*III-digested sequence) and 4 variable nucleotides were added to the 3' end of the adaptor sequence (Figure 2). For example, 1 primer set was as follows: forward primer, H1-1: 5'-AATTCGGCGCCGCGGATCCCCGGGG-3'; reverse primer H9-3: 5'-AATTCGGCGCCGCGGATCCCCAGGA-3' (the adaptor sequence is underlined, and the *Hae*III-digested sequence is shown in italics) (Figure 2).

We always used >12 primer sets and 0.83 μmol of each primer per cDNA library. PCR was performed with AmpliTaq Gold Master Mix (Applied Biosystems). The reaction mixture was heated at 95°C for 12 min, followed by 70 cycles of amplification. Each PCR cycle consisted of annealing and primer extension at 72°C for 30 s and denaturation at 94°C for 30 s. A single band was consistently obtained in ≈50% of the reactions. DNA was purified from the PCR by using MonoFas. Occasionally, we purified DNA fragments from the gels when >2 bands were detected. Direct sequencing was performed with the forward primer, reverse primer, or both.

When the number of viral particles in the sample was high, we omitted the RNase A and DNase I treatments and used the RNeasy Mini Kit (Qiagen) for RNA extraction. We occasionally used a whole transcriptome amplification kit (Rubicon Genomics Inc, Ann Arbor, MI, USA) instead of the WGA kit because both kits yielded similar amplification results.

In preliminary studies that used referential RNA viruses, we attempted to determine the nucleic acid sequences of SARS coronavirus, mouse hepatitis virus, West Nile virus, Japanese encephalitis virus, and dengue virus type 2 in culture supernatants (10–100 μL) by using the RDV method. The percentages of positive fragments (number of fragments containing viral nucleic acid/total number of

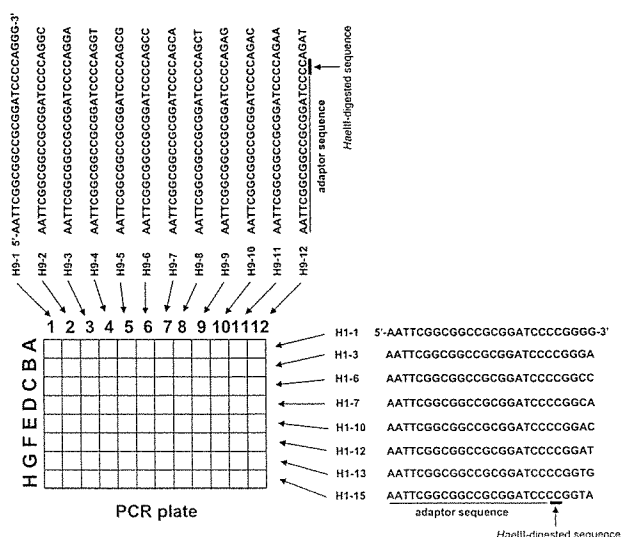


Figure 2. Primers used in rapid determination of viral RNA sequence method.

sequenced fragments) in the reactions for detection of these 5 viruses were 60% (3/5), 45% (5/11), 100% (12/12), 50% (5/10), and 40% (4/10), respectively. As a clinical application, a throat swab specimen from a patient with fever and upper respiratory infection was characterized. Although the specimen exhibited enterovirus-like cytopathic effect by inoculation into HEF and GMK cells when cell culture system for virus isolation was used (2), extracted RNA from the supernatant of the cells showed no amplification by reverse transcription-PCR (RT-PCR) when 1 of the conventional primer sets for human enteroviruses was used (3,4). In the cell culture supernatant analysis by the RDV method, the specimen exhibited amplification of the partial nucleotide sequences of coxsackie A14 virus (nucleotide sequence data are available in the DDBJ/EMBL/GenBank databases under accession nos. AB275848–AB275853). Thus, the RDV method could detect unidentified cytopathic-effect agents such as enterovirus that could not be detected by RT-PCR when the conventional primer set for enteroviruses was used.

## Conclusions

The RDV method is a rapid method for the direct determination of viral RNA sequences without using the cDNA cloning procedure. The limitations of the RDV method are the requirement for cell culture isolate and the large number of steps. However, RDV would be useful for species-independent detection of RNA viruses including unknown or untypeable emerging RNA viruses. Furthermore, with minor modifications, this method would also be applicable to the detection of DNA viruses and bacteria.

### Acknowledgments

We thank F. Taguchi and R. Watanabe for helpful discussions and M. Ogata for assistance.

This work was supported in part by the Japan Society for Promotion of Science, Tokyo, Japan.

Dr Mizutani is a senior researcher at the National Institute of Infectious Diseases, Tokyo, Japan. His current research focus is infectious disease surveillance by using new technologies.

2. Numazaki Y, Oahima T, Ohmi A, Tanaka A, Oizumi Y, Komatsu S, et al. A microplate method for isolation of viruses from infants and children with acute respiratory infections. *Microbiol Immunol.* 1987;31:1085-95.
3. Olive DM, Al-Mufti S, Al-Mulla W, Khan MA, Pasca A, Stanway G, et al. Detection and differentiation of picornaviruses in clinical samples following genomic amplification. *J Gen Virol.* 1990;71:2141-7.
4. Ishiko H, Shimada Y, Yonaha M, Hashimoto O, Hayashi A, Sakae K, et al. Molecular diagnosis of human enteroviruses by phylogeny-based classification by use of the VP4 sequence. *J Infect Dis.* 2002;185:744-54.

### References

1. Endoh D, Mizutani T, Kirisawa R, Maki Y, Saito H, Kon Y, et al. Species-independent detection of RNA virus by representational difference analysis using non-ribosomal hexanucleotides for reverse transcription. *Nucleic Acids Res.* 2005;33:e65.

Address for correspondence: Tetsuya Mizutani, Department of Virology 1, National Institute of Infectious Diseases, Gakuen 4-7-1, Musashimurayama City, Tokyo 208-0011, Japan; email: tmizutan@nih.go.jp

**EMERGING  
INFECTIOUS DISEASES**

A Peer-Reviewed Journal Tracking and Analyzing Disease Trends

Vol. 8, No. 5, May 2002

Search past issues of EID at [www.cdc.gov/eid](http://www.cdc.gov/eid)



## Oligomerization of Hepatitis C Virus Core Protein Is Crucial for Interaction with the Cytoplasmic Domain of E1 Envelope Protein<sup>∇</sup>

Kousuke Nakai,<sup>1</sup> Toru Okamoto,<sup>1</sup> Tomomi Kimura-Someya,<sup>2</sup> Koji Ishii,<sup>2</sup> Chang Kweng Lim,<sup>1</sup> Hideki Tani,<sup>1</sup> Eiko Matsuo,<sup>1</sup> Takayuki Abe,<sup>1</sup> Yoshio Mori,<sup>1</sup> Tetsuro Suzuki,<sup>2</sup> Tatsuo Miyamura,<sup>2</sup> Jack H. Nunberg,<sup>3</sup> Kohji Moriishi,<sup>1</sup> and Yoshiharu Matsuura<sup>1\*</sup>

*Department of Molecular Virology, Research Institute for Microbial Diseases, Osaka University, Osaka,<sup>1</sup> Department of Virology II, National Institute of Infectious Diseases, Tokyo,<sup>2</sup> Japan, and Montana Biotechnology Center, The University of Montana, Missoula, Montana 59812<sup>3</sup>*

Received 9 June 2006/Accepted 28 August 2006

Hepatitis C virus (HCV) contains two membrane-associated envelope glycoproteins, E1 and E2, which assemble as a heterodimer in the endoplasmic reticulum (ER). In this study, predictive algorithms and genetic analyses of deletion mutants and glycosylation site variants of the E1 glycoprotein were used to suggest that the glycoprotein can adopt two topologies in the ER membrane: the conventional type I membrane topology and a polytopic topology in which the protein spans the ER membrane twice with an intervening cytoplasmic loop (amino acid residues 288 to 360). We also demonstrate that the E1 glycoprotein is able to associate with the HCV core protein, but only upon oligomerization of the core protein in the presence of tRNA to form capsid-like structures. Yeast two-hybrid and immunoprecipitation analyses reveal that oligomerization of the core protein is promoted by amino acid residues 72 to 91 in the core. Furthermore, the association between the E1 glycoprotein and the assembled core can be recapitulated using a fusion protein containing the putative cytoplasmic loop of the E1 glycoprotein. This fusion protein is also able to compete with the intact E1 glycoprotein for binding to the core. Mutagenesis of the cytoplasmic loop of E1 was used to define a region of four amino acids (residues 312 to 315) that is important for interaction with the assembled HCV core. Taken together, our studies suggest that interaction between the self-oligomerized HCV core and the E1 glycoprotein is mediated through the cytoplasmic loop present in a polytopic form of the E1 glycoprotein.

Hepatitis C virus (HCV) is the causative agent of chronic hepatitis C, leading to steatosis, cirrhosis, and hepatocellular carcinoma. It is estimated that over 170 million people are infected with HCV worldwide (5, 18, 37). HCV is an enveloped single-stranded plus-sense RNA virus in the *Hepacivirus* genus of the family *Flaviviridae*, which also includes the flaviviruses and pestiviruses (36). The genome of HCV encodes a polyprotein of approximately 3,000 amino acids which is cotranslationally and posttranslationally processed to generate at least 10 viral proteins (12). The structural proteins, the core and E1 and E2 envelope glycoproteins, are encoded in the N-terminal portion of the polyprotein, and the nonstructural proteins, thought to be required for replication of the viral genome, are encoded in the C-terminal region (11). The core protein, which interacts with viral RNA (47) to form the nucleocapsid, is liberated from the N terminus of the polyprotein by signal peptidase cleavage in the downstream E1 protein (at position 191), and the C-terminal transmembrane region of the core protein (residue 164 to 191) is further cleaved at residues 177 or 179 by the signal peptide peptidase (16, 43). The remaining hydrophobic region of the core protein (domain II; residues 119 to 174) has been shown to affect the efficiency of signal peptide peptidase cleavage and the intracellular localization of core protein (14, 44). Although the C-terminal transmembrane

region of core protein and E1 were reported to interact with each other within the intramembrane space (25), the central hydrophobic region from residues 119 to 152 within domain II was also suggested to be responsible for the interaction between core and E1 (27).

Recently, *in vitro* replication of a JFH1 clone of HCV genotype 2a derived from a patient with fulminant hepatitis C was reported in a cell line that had been cured of its HCV replicon by treatment with interferon (23, 50, 51). However, this reverse genetics system is limited to the JFH-1 clone of genotype 2a and specific cell lines. Robust and reliable *in vitro* replication of other major genotypes of HCV such as genotypes 1a and 1b has yet to be developed. So far, biological functions of HCV envelope proteins have been characterized by using recombinant envelope proteins expressed *in vitro*, HCV-like particles produced in insect cells, and the pseudotyped virions based on vesicular stomatitis virus and retroviruses (8). The HCV polyprotein precursor must be specifically threaded through the membrane of the endoplasmic reticulum (ER) to undergo maturation to form the mature envelope glycoproteins (7). In the polyprotein, the C-terminal regions of E1 and E2 each contain a membrane-spanning domain as well as the hydrophobic signal peptide of the downstream viral protein (E2 and p7, respectively). These domains form hairpin structures that pass through the membrane twice, to allow processing by signal peptidase in the ER lumen. Upon signal peptidase cleavage, the C termini are thought to translocate into the cytoplasm to generate the type I membrane topology of the mature glycoproteins. The mature E1 and E2 glycoproteins

\* Corresponding author. Mailing address: Department of Molecular Virology, Research Institute for Microbial Diseases, Osaka University, 3-1, Yamadaoka, Suita, Osaka 565-0871, Japan. Phone: 81-6-6879-8340. Fax: 81-6-6879-8269. E-mail: matsuura@biken.osaka-u.ac.jp.

<sup>∇</sup> Published ahead of print on 13 September 2006.

remain noncovalently associated, interacting in part through their C-terminal transmembrane domains, which also mediate retention of the E1-E2 complex in the ER. Based on this model of membrane topology, the HCV envelope glycoproteins possess little or no cytoplasmic region. However, a physical association between E1 and the cytosolic core protein has been reported (25, 27), suggesting that the E1 glycoprotein is able to expose a cytoplasmic domain of sufficient length to interact with the core. In addition, the presence of the core protein has been shown to affect the folding of E1 (32).

We have previously suggested that the E1 glycoprotein may adopt a polytopic (double membrane-spanning) topology that coexists with the dominant type I form (35). In this study, we provide genetic evidence for a polytopic form of the E1 glycoprotein and for exposure of a centrally located cytoplasmic domain. Furthermore, we show that the cytoplasmic region of the polytopic form of E1 is required for interaction with amino acid residues 72 to 91 of the core protein.

#### MATERIALS AND METHODS

**Cell culture.** 293T cells were maintained in Dulbecco's modified Eagle's medium (Sigma, St. Louis, MO) containing 2 mM L-glutamine, penicillin, and streptomycin and supplemented with 10% fetal bovine serum.

**Plasmids.** A cDNA of E1 glycoprotein was amplified from HCV type 1b strain J1 (1) by PCR using *Pfu* Turbo DNA polymerase (Stratagene, La Jolla, CA) and inserted between *NheI* and *BamHI* sites of pJW4303, which contains the signal sequence of tissue plasminogen activator and the bovine growth hormone polyadenylation signal (a kind gift from J. M. Mullins), to generate pJW383. For the deletion analysis, the plasmids pJW360 and pJW288 encoding residues 192 to 360 and 192 to 288, respectively, were amplified by PCR and cloned into pJW4303. The plasmids pJW383d1 and pJW383d2, containing deletions in residues 261 to 286 and 289 to 340, respectively, were generated from pJW383 by splicing of overlapping extensions (13, 15) as described previously (44). A cDNA fragment encoding core to E2 proteins of HCV strain J1 was amplified by PCR and cloned into pCAGGs-PUR (28), and glycosylation site mutations in the E1 protein were generated by the method of splicing by overlapping extension. For the yeast two-hybrid assay, pGBKT7HCVCore173 was used as bait, as described previously (38). The gene encoding amino acids 288 to 346 of HCV E1 protein was amplified from cDNA of strain J1 and introduced into *NdeI* and *EcoRI* sites of a pGADT7 vector (Clontech, Palo Alto, CA). In the same way, deletion mutants of core protein encoding residues 1 to 151, 1 to 25, 24 to 173, 38 to 173, 58 to 173, 72 to 173, and 92 to 173 were amplified by PCR and cloned into a pGBKT7 vector. The FLAG sequence was introduced between amino acids 195 and 196 of the cDNA encoding residues 1 to 383 of the HCV polyprotein and replaced Ala<sup>383</sup> with Arg to avoid processing by signal peptidase and spacer amino acids (Gly-Gly-Gly-Ser), and influenza virus hemagglutinin (HA) sequence was added at the C terminus. The resulting cDNA fragment encoding core protein, FLAG tag, E1, and HA tag was cloned into a pcDNA3.1(+) vector and designated Flag-core-E1-HA (see Fig. 2D, below) and used for *in vitro* transcription and translation. Similarly, the FLAG sequence was introduced into the cDNA encoding residues 151 to 383 of the HCV polyprotein, and the HA sequence was added at the C terminus. The resulting cDNA fragment encoding the C-terminal hydrophobic/transmembrane region of the core protein, FLAG tag, E1, and HA tag was designated Flag-E1-HA (see Fig. 3A, below). The DNA fragments encoding residues 1 to 191 with amino acids 72 to 91 deleted were generated by splicing via overlapping extension and cloned into pCAGGS (CoreΔ72-91) (see Fig. 4A, below) (42). The DNA fragment encoding the cytoplasmic domain of the E1 protein with a C-terminal HA tag was amplified by PCR and introduced at *HindIII* and *SacII* sites of pEGFP-C3. pCAGGS plasmids encoding core to p7 replacing residues 304 to 307, 308 to 311, 312 to 315, 316 to 319, 320 to 323, 324 to 327, or 328 to 331 with Ala were generated by using splicing with overlapping extension (see Fig. 6A, below).

**Antibodies.** Mouse monoclonal antibody to HA tag (HA11) and anti-FLAG antibody (M2) were purchased from Covance (Richmond, CA) and Sigma, respectively. Mouse monoclonal antibodies to core protein (clones 11-7, 11-10, and 11-14) were gifts from S. Yagi (2). Anti-E1 mouse monoclonal antibody (clone 0726) was prepared by immunization using the membrane fraction of the

CHO L10 cell line, which constitutively expresses HCV envelope proteins (30). Anti-E2 monoclonal antibody (clone 187) was a generous gift from M. Kohara.

**Yeast two-hybrid assay.** A yeast two-hybrid assay was carried out by using Matchmaker system 3 (Clontech) according to the manufacturer's protocol. The bait vector pGBKT7HCVcore 173 (38) or empty plasmid was transfected into *Saccharomyces cerevisiae* strain AH109 together with the prey vectors, pGADT7-based constructs (see Table 1, below). The yeast cells possessing pGBKT7/p-53 and pGADT7/large T antigen were used as positive controls, while yeast cells possessing pGBKT7 and pGADT7 were the negative controls. These transfected yeast colonies were cultivated on dropout plates lacking Trp, Leu, His, and Ade (test plates) or plates lacking Trp and Leu (control plates) and then incubated at 30°C for 1 week.

**Transfection, immunoblotting, and immunoprecipitation.** Liposome-mediated DNA transfection using Lipofectamine 2000 (Invitrogen, Carlsbad, CA) was described previously (38). Transfected cells were cultured at  $2 \times 10^5$  cells/well in a six-well plate, harvested 30 to 48 h posttransfection, washed twice with phosphate-buffered saline (PBS), and incubated at 4°C for 30 min in 0.25 ml of lysis buffer (20 mM Tris-HCl [pH 7.4], 135 mM NaCl, 1% Triton X-100, and 10% glycerol supplemented with 1 mM phenylmethylsulfonyl fluoride, 50 mM NaF, and 5 mM Na<sub>3</sub>VO<sub>4</sub>). After freezing and thawing, lysed cells were centrifuged at 20,000 × *g* for 5 min. The resulting cleared lysate was stored at -80°C prior to use for immunoprecipitation and blotting. Immunoprecipitation was carried out according to the method described previously (44). Briefly, lysates were preincubated at 4°C for 5 h in the lysis buffer with or without 1 mM MgCl<sub>2</sub> and 0.1 mg/ml of yeast tRNA (Sigma) prior to immunoprecipitation. The resulting lysates (0.2 ml) were gently rotated with 1.0 μg of anti-FLAG, anti-HA, or mixed mouse monoclonal anti-HCV core antibodies or mouse monoclonal antibody to the E1 protein at 4°C for 3 h with or without 1 mM MgCl<sub>2</sub> and 0.1 mg/ml of yeast tRNA. The immunocomplex was gently rotated at 4°C for 3 h with 10 μl of 50% (vol/vol) protein G-Sepharose 4 Fast Flow beads (Amersham Pharmacia Biotech, Franklin Lakes, NJ) with or without 1 mM MgCl<sub>2</sub> and 0.1 mg/ml of yeast tRNA and then centrifuged at 20,000 × *g* for 30 s. The precipitated beads were washed five times with 0.5 ml of lysis buffer containing or lacking 1 mM MgCl<sub>2</sub> and 0.1 mg/ml of yeast tRNA and then boiled in 50 μl of the loading buffer. The boiled samples were subjected to sodium dodecyl sulfate-polyacrylamide gel electrophoresis. The proteins in gels were transferred to Immobilon-P polyvinylidene difluoride membranes (Millipore, Bedford, MA) and then blotted with primary antibody and secondary horseradish peroxidase-conjugated antibody. The immunocomplexes on membranes were visualized with Super Signal West Femo substrate (Pierce, Rockford, IL) and detected by using an image analyzer LAS-3000 (Fujifilm, Tokyo, Japan).

**Protease protection assay of HCV proteins synthesized by *in vitro* transcription/translation.** A plasmid encoding a FLAG-core-E1-HA protein was transcribed under the control of a T7 promoter by using the RiboMax large-scale RNA production system with Ribo m<sup>7</sup>G cap analog (Promega, Madison, WI). *In vitro* translation was carried out in the presence of [<sup>35</sup>S]methionine-cysteine (Amersham, Piscataway, NJ) by using rabbit reticulocyte lysate and canine pancreatic microsomal membrane (Promega). Translated sample was diluted sevenfold with PBS and then mixed with tosylsulfonyl phenylalanyl chloromethyl ketone-treated trypsin (Sigma) at a final concentration of 2 μg/ml. The mixture was incubated at 30°C for 60 min with or without 0.5% Nonidet P-40, and then soybean trypsin inhibitor (Sigma) was added at a final concentration of 20 μg/ml. Digestion products were immunoprecipitated with anti-FLAG antibody.

**Indirect immunofluorescence analysis.** 293T cells were washed with PBS at 40 h after transfection and fixed with 3% paraformaldehyde in PBS for 20 min at room temperature. The fixed cells were permeabilized with 0.2% Triton X-100 for 3 min at room temperature and blocked with nonfat milk solution. Cells were incubated with the anti-E1 antibody for 60 min at 37°C and then with fluorescein isothiocyanate-conjugated goat anti-mouse immunoglobulin G (IgG; TAGO, Burlingame, CA). HCV E1 protein was visualized by fluorescence microscopy (TE300; Nikon, Tokyo, Japan).

**Velocity sedimentation with sucrose gradients.** Transfected 293T cell were suspended in MNT buffer (20 mM 2-morpholinoethanesulfonic acid, 100 mM NaCl, 30 mM Tris-HCl [pH 8.6], and 0.1% Triton X-100) and then incubated at 4°C for 5 h with or without 0.1 mg/ml of yeast tRNA and 1 mM MgCl<sub>2</sub>. Each sample was layered on top of 12 ml of sucrose with a 20 to 60% gradient and then centrifuged in a Beckman SW 41Ti rotor (Beckman Coulter, Tokyo, Japan) at 30,000 rpm for 3 h at 4°C. Centrifuged lysates were collected from the bottoms of the tubes and then concentrated with trichloroacetic acid. After washing with ethanol, concentrated proteins were subjected to SDS-PAGE and immunoblotting.

## RESULTS

**Prediction of the topology of the E1 protein in the membrane.** Although a small fraction of the HCV envelope glycoproteins expressed in 293T cells is translocated onto the plasma membrane (3), the vast majority of E1 is retained in the ER membrane (6). Previously, we showed that both a central hydrophobic region of E1 (residues 260 to 288) and the C-terminal hydrophobic region (residues 360 to 383) are important for ER retention (29). As in the C-terminal hydrophobic region, the amino acid sequence of the central hydrophobic region is highly conserved among HCV isolates (4). To investigate the role of these two hydrophobic regions in the biogenesis of the E1 glycoprotein, we utilized the TMHMM algorithm (19), a computer program trained to identify potential transmembrane helical regions. The algorithm identified both hydrophobic regions as having a high probability of transmembrane helix (Fig. 1A). To examine the function of the hydrophobic regions as transmembrane domains, we constructed a series of deletion mutants in the E1 protein in which one or the other of the hydrophobic segments was absent (Fig. 1B). Mutant E1 glycoproteins were expressed in 293T cells, and the cellular localization of E1 proteins was determined by indirect immunofluorescence analysis (Fig. 1B). The full-length E1 (383) was detected only in permeabilized cells, consistent with its retention in the ER. The 383d2 mutant, which contains both hydrophobic regions but lacks the intervening hydrophilic region (residues 289 to 340), was also detected in the cytoplasm but not on the cell surface as the full-length E1. By contrast, deletion mutants lacking the central (383d1) or C-terminal (288 and 360) hydrophobic domains were detected on the cell surface in nonpermeabilized cells, suggesting that both the central and the C-terminal hydrophobic domains are required for retention of the E1 protein on the ER membrane. If the central hydrophobic domain traverses the ER membrane as predicted by the TMHMM program, the region between positions 288 and 360 would be expected to lie in the cytoplasmic space. Based on this model and on the results with E1 deletion mutants, we suggest that the E1 protein might be able to retain two membrane topologies: the conventional type I topology and a polytopic topology that spans the membrane twice with N and C termini in the ER lumen and an intervening cytoplasmic loop, as reported previously (35) (Fig. 1C). Recently, a similar polytopic form of the fusion glycoprotein of Newcastle disease virus was identified (31).

**Mutational analysis of putative N-glycosylation sites of the E1 glycoprotein.** To explore the membrane topologies of E1, we examined the utilization of potential glycosylation sites. The E1 protein of HCV strain J1 (1) contains seven N-glycosylation sequence motifs (Asn-X-Ser/Thr) at amino acid positions 196, 209, 233, 234, 250, 305, and 325 (Fig. 2A). The Asn residues at these possible N-glycosylation sites were individually replaced with Gln, and the mutant E1 glycoproteins were expressed as a core-, E1-, or E2-containing polyprotein in 293T cells. In all cases, the mutant polyproteins were expressed and properly processed by signal peptidase and signal peptide peptidase to generate the core, E1, and E2 proteins (Fig. 2B). The mutant E1 proteins displayed distinct glycoforms consistent with changes in glycosylation. The wild-type E1 glycoprotein exhibited a major band of 34 kDa and a minor band of 32 kDa.

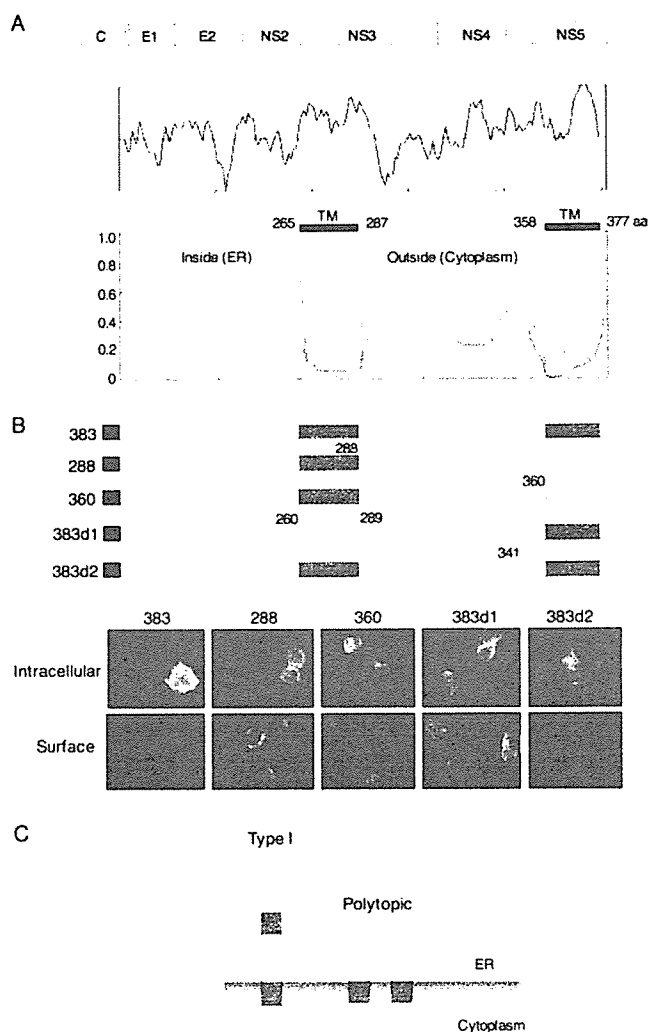


FIG. 1. Prediction of the membrane topology of the E1 protein. (A) Genome structure of HCV and a hydrophobic profile of the amino acid sequence of the E1 protein are shown at the top. The transmembrane helices in the E1 protein were predicted by the TMHMM program (19), and regions of high probability (amino acid residues 265 to 287 and 358 to 377) are indicated. (B) 293T cells transfected with the wild type (383) and deletion constructs were fixed with paraformaldehyde and permeabilized with Triton X-100 (intracellular) or not permeabilized (surface). E1 proteins were visualized with an anti-E1 monoclonal antibody and fluorescein isothiocyanate-conjugated anti-mouse IgG. (C) Possible topologies of the E1 protein on the ER. (Left) Type I topology model possessing a C-terminal transmembrane region; (right) a polytopic topology that spans the membrane twice, with both N and C termini in the ER lumen and with an intervening cytoplasmic loop.

The 325 mutant was unchanged from the wild-type E1, suggesting that the 325 position is not utilized, presumably due to an unfavorable NWSP motif in the genotype 1a protein (33). The 209, 233/234, and 250 mutants migrated faster than the authentic E1 protein and exhibited two bands of 32 and 30 kDa. The E1 of the 196 mutant was apparently not recognized by the monoclonal antibody directed to the N-terminal region of E1. In the 233 and 234 mutants, glycosylation occurred at the remaining Asn (234 or 233, respectively). These mutants comigrated with the wild-type E1 glycoforms, suggesting that

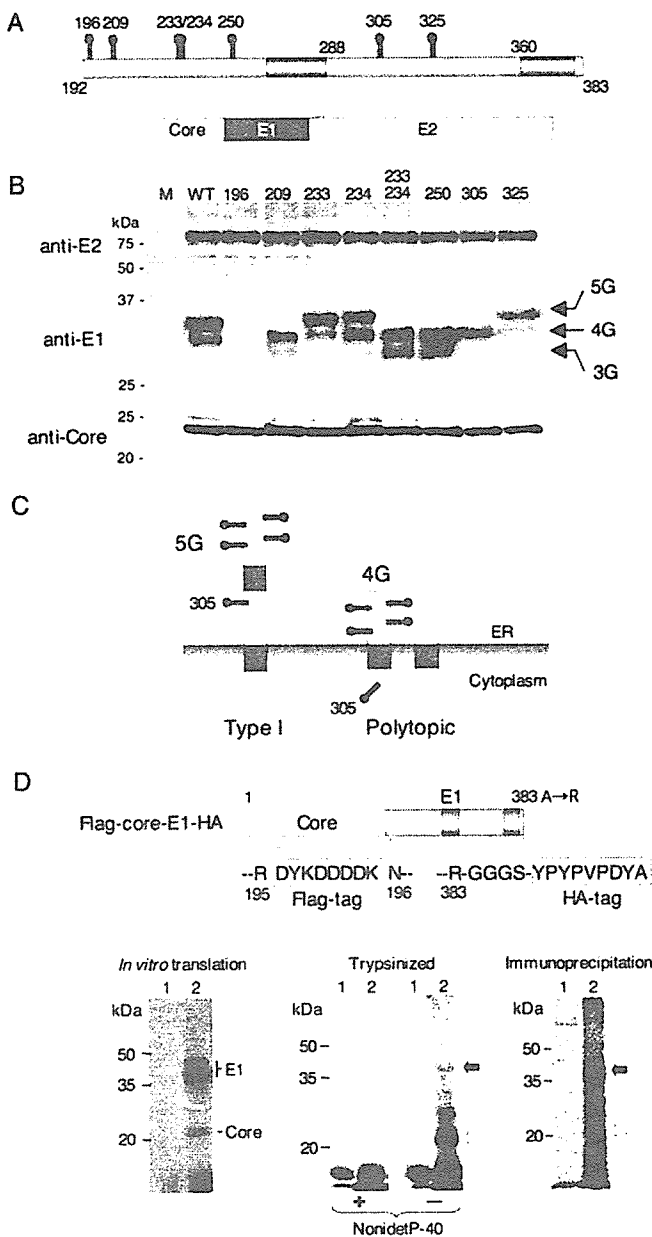


FIG. 2. Mutational analysis of N-glycosylation sites and protease protection assay of the E1 protein. (A) Positions of potential N-glycosylation sites (gray and black spikes) in the E1 protein are shown. (B) Asn residues in the possible N-glycosylation sites in the E1 protein were individually replaced with Gln. Mutant plasmids encoding the core, E1, and E2 polyproteins (A) were expressed in 293T cells, and processed core, E1, and E2 proteins were detected by immunoblotting. (C) Type I and polytopic topology models of E1 proteins bearing carbohydrates at positions of 196, 209, 234, 250, and 305 (5G) and 196, 209, 234, and 250 (4G), respectively. The 305 mutant would exhibit a single band of 4G irrespective of the topologic models. (D) Structure of the FLAG-core-E1-HA construct encoding the HCV core and E1 polyprotein carrying FLAG and HA tags in the N- and C-terminal regions of the E1 protein (top). (Bottom, left) In vitro translation of capped RNA transcribed from the FLAG-core-E1-HA (lane 2) and without RNA (lane 1) in the presence of [ $^{35}$ S]methionine-cysteine using rabbit reticulocyte lysate and canine pancreatic microsomal membrane. (Bottom, middle) Translated products of FLAG-core-E1-HA (lane 2) and without RNA (lane 1) were digested with trypsin in the presence (+) or absence (-) of 0.5% Nonidet P-40. (Bottom, right) Digestion products were immunoprecipitated with control (lane 1) and anti-FLAG (lane 2) antibody. Black and white arrows indicate protected and digested E1 protein, respectively.

only one or the other of the overlapping motifs can be utilized in the wild-type molecule. Glycosylation in this region was absent in the double mutant (233/234). The existence of two glycoforms of E1 may reflect incomplete and stochastic use of the available glycosylation sites or, alternatively, the presence of two discrete topological forms of E1 protein. For instance, the major band of 34 kDa in the wild-type glycoprotein might correspond to the type I topology form, with glycosylation at 196, 209, 234, 250, and 305 (5G), whereas the minor band of 32 kDa might correspond to the polytopic form of E1, bearing glycans at positions 196, 209, 234, and 250 (4G). In this regard, it is noteworthy that the 305 mutant of E1 exhibited only a single band of 32 kDa. The absence of a second glycoform is consistent with the putative cytoplasmic localization of Asn305 in a polytopic form of E1 (Fig. 2C). Taken together, this mutational analysis provides support to the model in which the HCV E1 glycoprotein is able to exist in either the type I or polytopic form. In the latter form, an extended cytoplasmic domain in E1 would be available to interact with the core protein in the virion.

**Protease protection assay of the E1 protein.** To confirm the presence of the cytoplasmic domain in the E1 protein, in vitro translation products of the HCV core and E1 polyprotein carrying FLAG and HA tags in the N- and C-terminal regions of the E1 protein, respectively, were digested with trypsin, and the protected portion of the E1 glycoprotein was immunoprecipitated by anti-FLAG antibody. As shown below in Fig. 4D, treatment of the translation products with trypsin in the presence of Nonidet P-40 resulted in complete digestion, and a 22-kDa band (major) and several <35-kDa faint bands were detected in the absence of the detergent. When in vitro-translated HCV core protein was treated similarly, no band was detected, irrespective of the presence of detergent (data not shown); therefore, the protected bands from trypsin digestion were derived from the E1 protein. Although the 22- to 35-kDa bands were specifically immunoprecipitated with anti-FLAG antibody but not with control antibody, the 35-kDa protein corresponding to the type I topology of the E1 protein resistant to trypsin digestion was dominant. This might be due to the difference in the reactivity of the anti-FLAG antibody, which recognizes the intact E1 protein more efficiently than digested ones. These results further support the presence of the polytopic form of HCV E1 glycoprotein, which has a cytoplasmic region together with a type I topology in the ER.

**HCV core protein binds to the E1 protein in the presence of tRNA.** The HCV core protein undergoes extensive conformational changes upon binding to nucleic acid and self-assembling into nucleocapsid-like particles (20). To investigate the effects of nucleic acid on oligomerization of the core protein, lysates of 293T cells expressing HCV core protein were incubated in the presence or absence of yeast tRNA (20) and subjected to velocity sedimentation in a sucrose gradient. Oligomerized core protein was detected in fractions 1 to 4 in the presence of tRNA but not in those in the absence of tRNA (Fig. 3A). To specifically examine the interaction between HCV core and E1 proteins in the assembly of the nucleocapsid-like particles, we coexpressed the core protein with an E1 protein possessing a FLAG tag near its N terminus and an HA tag at the C terminus (Flag-E1-HA) (Fig. 3B, left). The transfected cells were lysed with Triton X-100, and the E1 protein